

Inelastic collisions involving excited cesium atoms at thermal energies

J. Cuvellier, P. R. Fournier, F. Gounand, J. Pascale, and J. Berlande

Centre d'Etudes Nucléaires de Saclay, Service de Physique Atomique-BP No.2, 91190-Gif-sur-Yvette, France

(Received 29 July 1974)

Cross sections for the $7P_{1/2} \rightarrow 6D_{3/2}$ and $7P_{3/2} \rightarrow 6D_{3/2}$ transitions, induced at thermal energies by cesium-rare-gas collisions, have been measured over the temperature range from 420 to 615 K. The values of the cross sections are found to be surprisingly high when considering only the energy defect of the levels involved. Moreover, the cross sections for Cs-He collisions exhibit very different behavior than those corresponding to heavier rare gases. A discussion with the aid of theoretical adiabatic potential curves explains the main features of the experimental results. Theoretical calculations of the cross sections have been carried out for some cases, and give results in satisfactory agreement with the experimental values.

I. INTRODUCTION

Recent experimental and theoretical work on inelastic atomic collisions at thermal energies involving highly excited atoms is of great interest in efforts to obtain a better knowledge of interatomic forces.¹⁻³

Numerous experiments⁴ have been performed on the transfer of excitation between the fine-structure levels of the first 2P doublet of the alkali metals when they undergo a collision with a rare-gas atom, i.e.,

$$A(^2P_{1/2}) + X \xrightleftharpoons[Q']{Q} A(^2P_{3/2}) + X - \Delta E,$$

where A is an alkali-metal atom, ΔE the fine-structure splitting, X is a rare-gas atom in its ground state, and Q and Q' are the cross sections associated with these processes. The general feature clearly shown by the experimental results is that Q and Q' are directly related to the magnitude of ΔE . However, for a better understanding of these inelastic processes a study of higher excited levels was necessary. For this reason fine-structure transitions in the second and third 2P doublets of cesium, induced by collisions with rare-gas atoms, have been studied in our laboratory.^{1,5} The results have shown that the absolute values of the cross sections depend not only on the energy defect ΔE but also on the position of the doublet with respect to the other levels in the cesium energy diagram (Fig. 1). It has been suggested that coupling with neighboring levels might occur.³

A reliable theoretical computation of these collisional cross sections has been done only for the first resonant doublet of the lightest alkali metals. In that case the simplified potential-energy curves used in the calculations seem to be correct in the range of internuclear distances where the transitions are the most probable.⁶⁻⁸

No agreement was obtained with similar calculations for collisions involving higher excited states.³ In view of these results it is obvious that the theoretical calculation of the cross sections requires a fairly good knowledge of the adiabatic potential curves of the alkali-rare-gas atom pairs. In a recent calculation of the alkali-rare-gas adiabatic potentials the importance of coupling between neighboring levels, giving rise to structure in the potential-energy curves, was clearly pointed out.^{9,10} An examination of the curves suggests, in particular, that an experimental study of extra-multiplet collisional transitions between the 7^2P and 6^2D levels of cesium is of interest. The potential curves asymptotically correlated to these levels show a pronounced structure due to coupling between these levels.

The possibility, for the first time, of comparing theoretical predictions with experimental results has led us to complete our previous investigation of intramultiplet transitions concerning the second resonant doublet of cesium with the experimental study of the ($7^2P \rightarrow 6^2D$) transitions. In this article we report on the experiment and discuss the results with the help of the potential-energy curves.

II. DESCRIPTION OF EXPERIMENT

A. Method

We are concerned with the collisional process

$$\text{Cs}(j) + X \xrightleftharpoons[Q_{ij}]{Q_{ji}} \text{Cs}(i) + X - \Delta E, \quad (1)$$

where X is a rare-gas atom in its ground state and ΔE is the energy defect between the j and i excited levels. The cross section for the transfer of excitation from j to i is denoted by Q_{ji} ; the reverse by Q_{ij} . Figure 2 shows the levels involved in the process: In our case the in-going channel is either the $7^2P_{1/2}$ or $7^2P_{3/2}$ level. The population of these

levels is achieved by photoexcitation from the ground state ($6^2S_{1/2}$ level) using a pulsed dye laser. The measurement of the intensities of two lines originating from the levels j (direct fluorescence) and i (sensitized fluorescence) by a photon-counting technique allows us to determine the population ratio of these two levels as a function of the rare-gas pressure. The cross sections Q_{ji} and Q_{ij} are then derived (see Sec. III B). The experimental setup, shown in Fig. 3, consists of three main parts: the dye laser, the fluorescence cell, and the detection system.

B. Dye laser

We use a pulsed dye laser because no cw dye laser operating at the required wavelengths (4555 and 4593 Å) was commercially available at the start of this experiment. A water-cooled flash lamp achieves the pumping of the dye (4, 6 dimethyl, 7 methyl amino coumarin). By inserting a Fabry-Perot interferometer in the cavity we obtain a laser linewidth of about 1 Å. By rotation of the interferometer we can tune the wavelength over a large spectral range, providing selective excitation of the two 7^2P -doublet components. The laser pulses have a half-width time duration of about 1.5 μsec and a maximum output power of 50 μJ per pulse. The repetition rate is 3 Hz. An optical system using a cesium vapor lamp ensures control of the laser wavelength. Because of the well-known poor power and wavelength stability of the dye laser pulses, we use an appropriate detection system.

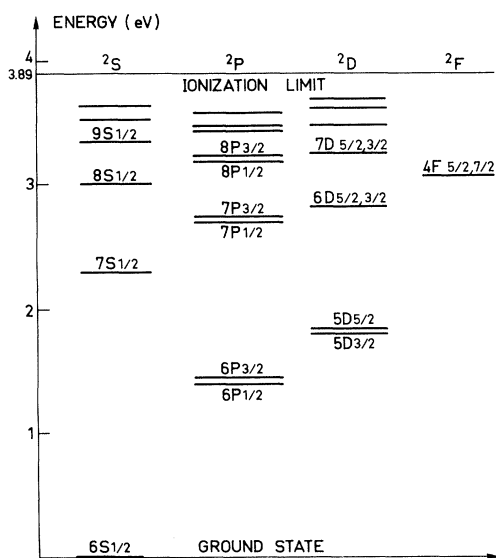


FIG. 1. Energy-level diagram of cesium.

C. Fluorescence cell

The fluorescence light is observed at a right angle to the exciting laser beam. The form of the cell and the material used (suprasil 1) ensure a minimum of stray light. The well-defined position of the laser beam allows us to determine the optical path of the fluorescence light, which is an important parameter for the calculation of possible light-absorption effects. The temperature of the oven in which the fluorescence cell is set can be varied over the range 400–630 K. The liquid cesium is located in a sidearm, the temperature of which is kept at a fixed value by a separate heating system. Thermocouples ensure the measurements and the regulation of the temperature in the whole system. The fluorescence cell is connected by a capillary to a vacuum or gas filling system. After a typical baking procedure the residual pressure is about 10^{-6} Torr. The rare-gas pressure is measured with an oil manometer. A liquid-nitrogen-cooled trap and, for the helium case, a cataphoresis tube permit further purification of the rare gas before its introduction into the fluorescence cell.

D. Detection system

Intensity fluctuations of the excitation source require simultaneous measurement of the direct and sensitized fluorescence. A short-focal-length lens allows the observation of a small interaction region in the cell. The direct fluorescent light, possibly attenuated by a neutral density filter, is analyzed with an interference filter. The sensitized fluorescence light is focused on the entry slit of a grating monochromator. The measurements are then achieved by using (i) a high-speed cooled photomultiplier (pulse duration <5 nsec) of 56 DVP or C 31034 type, and (ii) a 100-MHz detection system (amplifier, discriminator, and scaler). A

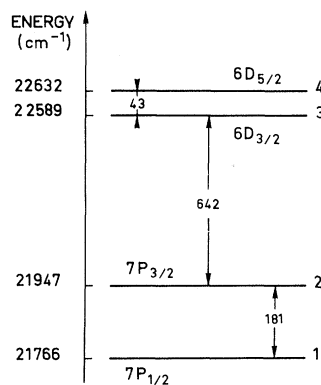


FIG. 2. Energy levels involved in this experiment.

trigger system opens the counter during a time greater than the light-pulse duration, but sufficiently short to ensure a very low dark-noise level. Preliminary experiments permit the calibration of the whole system.

III. DATA ANALYSIS

The cross sections for excitation transfer are obtained after a two-step procedure. First, from the experimental results of the intensity ratio of sensitized to direct fluorescence light the ratios of the i - to j -level populations are deduced as a function of the rare-gas pressure. Then the cross sections are determined from the population ratios by using a four-level coupling model.

A. Determination of population ratios

The counting measurements are made in pulsed mode, with a pulse-time duration greater than the lifetimes of the studied excited levels. The counting apparatus operates during a time τ which covers completely the excitation light pulse. If $\mathcal{N}(j)$ is the instantaneous population of atoms lying in the j level, $N(j) = \int_0^\tau \mathcal{N}(j) dt$ represents the total number of atoms lying in the j level during the laser pulse and $A_{j \rightarrow k} N(j)$ is the total number of photons spontaneously emitted in the transition from the level j to the level k (where $A_{j \rightarrow k}$ is the Einstein coefficient). The detection system, tuned to the $j \rightarrow k$ transition, gives a counting signal $C(j)$ proportional to $A_{j \rightarrow k} N(j)$. In the same way, we obtain for the $i \rightarrow l$ transition a counting signal $C(i)$ proportional to $A_{i \rightarrow l} N(i)$.

We can write

$$\frac{N(i)}{N(j)} = \frac{A_{j \rightarrow k}}{A_{i \rightarrow l}} X_j Y_{ij} \frac{\alpha C(i)}{\beta C(j)}, \quad (2)$$

where Y_{ij} represents the relative efficiency of the whole detection apparatus, taking into account the attenuation of the beams, the geometrical arrangement of the two detection channels, and their relative sensitivity. X_j takes into account the influence of light absorption. The quantities α and β are corrective factors for the evaluation of the real counting rate when the dead time of the electronic apparatus is taken into account (the dead time has been previously found to be 10 nsec).

The determination of Y_{ij} is achieved by appropriate experiments. Measurements are performed with the sidearm containing liquid cesium at a temperature of 90°C. This corresponds to a cesium pressure of about 3×10^{-4} Torr [we use Nottingham's formula¹¹]. Because the optical path of the fluorescence light is about 3 mm, the absorption of the direct fluorescence ($7^2P_{1/2} \rightarrow 6^2S_{1/2}$ or $7^2P_{3/2} \rightarrow 6^2S_{1/2}$ transition) is not negligible as it is in the case for the sensitized fluorescence ($6^2D_{3/2} \rightarrow 6^2P_{1/2}$ transition). We calculate the X_j coefficient using the results given by Refs. 12-14, including, when necessary, in our calculation the pressure broadening of the cesium lines by the rare gas. The calculated value of X_j does not differ from unity by more than 20%.

We used in our calculations the A values given by Warner.¹⁵ The choice of A values will be discussed later (see Sec. III C 4). The measurements of the rare-gas pressure, using an oil manometer, need correction because of thermal transpiration, the manometer not being at the same temperature as the fluorescence cell. Knowledge of the flow regime (molecular, viscous, or intermediate) allows us, by an interpolation method, to determine the corrective factor under the experimental conditions.^{16, 17}

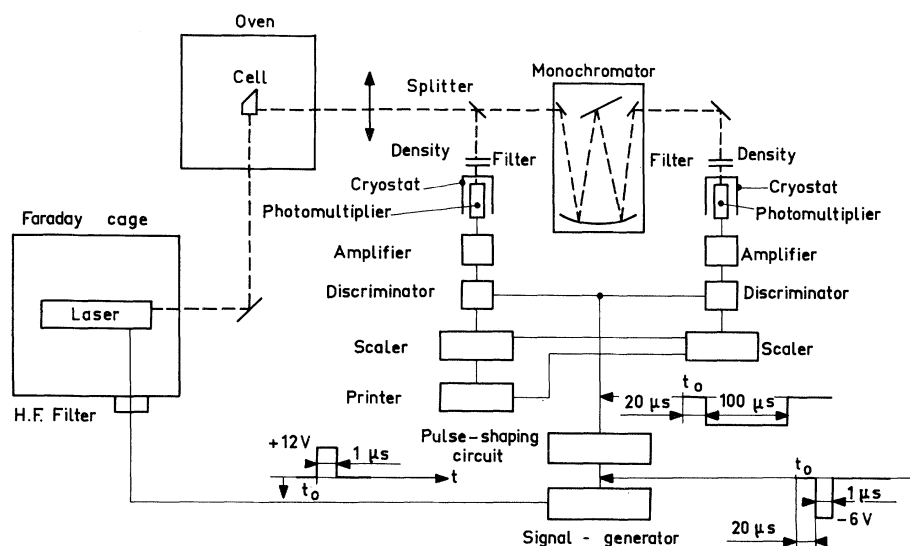


FIG. 3. Experimental setup.

B. Derivation of cross sections

The results of the previous experiments concerning intramultiplet transitions induced in alkali-rare-gas collisions are, in general, interpreted using a two-level scheme [i.e., j and i levels of Eq. (1)]. This scheme is well justified in the case of the first resonant doublet but must be modified in the case of higher excited levels because of the influence of other neighboring levels on the population ratios. We will describe here a more general model which allows us to analyze the experimental data when one has to consider the influence of a great number of levels. We will then apply the results obtained to the case of the $7^2P_{1/2, 3/2}$ and $6^2D_{3/2, 5/2}$ levels involved in this study (these four levels are well separated from the others in the energy diagram of cesium).

Let us consider a large number of atomic levels i, j, \dots . The following processes are supposed to couple these levels:

(a) Collisional processes. These are characterized by a frequency K_{ji} with $K_{ji} = N_g \bar{v} Q_{ji}$, where N_g is the rare-gas pressure, \bar{v} the mean velocity of the relative motion of the colliding particles, and Q_{ji} is the Maxwellian averaged cross section for the $j \rightarrow i$ collisional transition considered.

(b) Radiative processes. These are characterized by the Einstein coefficients A_{ji} (some of them equal to zero).

(c) Photoexcitation processes. These are denoted by ϕ_{ji} . These terms represent radiative pumping due to the cell considered as a black body.

We can write the population balance of the level i in the form

$$\sum_{p \neq i} N(p)(K_{pi} + A_{pi} + \phi_{pi}) = N(i) \sum_{p \neq i} (K_{ip} + A_{ip} + \phi_{ip}) \\ = N(i)(K_i + A_i + \phi_i),$$

with

$$\sum_{p \neq i} K_{ip} = K_i, \quad \sum_{p \neq i} A_{ip} = A_i, \quad \sum_{p \neq i} \phi_{ip} = \phi_i.$$

$N(i)$ and $N(p)$ are, as defined previously, the integrated populations of levels (i) and (p) during the measurement time τ .

Denote the photoexcited level by j , the level corresponding to the sensitized fluorescence by i , and the ratio $N(k)/N(l)$ by R_{kl} . We can write, using the preceding formula,

$$R_{ij} = \sum_{p \neq i} R_{pj} \alpha_{pi}, \quad (3)$$

$$\alpha_{pi} = (K_{pi} + A_{pi} + \phi_{pi}) / (K_i + A_i + \phi_i). \quad (4)$$

Note, finally, that the principle of detailed balancing can be written

$$(R_{ij})_{\text{eq}} = \left(\frac{K_{ji}}{K_{ij}} \right)_{\text{eq}} = \frac{Q_{ji}}{Q_{ij}} = \frac{g_i}{g_j} e^{(-\Delta E_{ij}/kT)}, \quad (5)$$

where g_i and g_j are the statistical weights of the i and j levels, ΔE_{ij} is the energy defect between these two levels, and the eq subscript indicates that the corresponding quantities are defined at Boltzmann equilibrium at the gas temperature T .

Applying this model to the four levels $7^2P_{1/2, 3/2}$ and $6^2D_{3/2, 5/2}$ and using the notation of Fig. 2, Eq. (3) can be written

$$R_{31} = \alpha_{13} + R_{21} \alpha_{23} + R_{41} \alpha_{43}.$$

Since $R_{41} = R_{43} R_{31}$, one obtains

$$R_{31} = (\alpha_{13} + R_{21} \alpha_{23}) / (1 - R_{43} \alpha_{43})$$

and, finally, using Eq. (4),

$$R_{31} = \frac{(K_{13} + \phi_{13}) + R_{21}(K_{23} + \phi_{23})}{K_3 - R_{43}K_{43} + A_3}.$$

A similar expression can be obtained for R_{32} .

The experiment determines R_{31} (and R_{32}) as a function of the rare-gas pressure N_g (note, in particular, that $\phi_{13} = R_{31} A_3$ when $N_g = 0$). Previous measurements (5) determine R_{21} (and R_{12}) as a function of N_g . The above formula can now be written

$$R_{31} = \frac{(N_g \bar{v} Q_{13} + \phi_{13}) + R_{21}(N_g \bar{v} Q_{23} + \phi_{23})}{N_g \bar{v} (Q_3 - R_{43} Q_{43}) + A_3}, \quad (6)$$

where Q_3 is the total collisional depopulation cross section of level 3.

The preceding analysis omits the influence of (Cs-Cs) collisions. Strictly speaking, the collisional frequency K_{ji} must be written

$$K_{ji} = N_g \bar{v} Q_{ji} + N_{Cs} \bar{v}_{Cs} Q_{jiCs}$$

N_{Cs} is the cesium density, \bar{v}_{Cs} is the mean velocity of the relative motion of two colliding cesium atoms, and Q_{jiCs} is the Maxwellian averaged cross section for the $j \rightarrow i$ transition induced by (Cs-Cs) collisions. In our experiment the cesium density N_{Cs} is kept at a fixed value. The effects of (Cs-Cs) collisions in Eq. (6) are (i) introduction into the numerator of two constant terms which can be regarded as included in the experimental values of ϕ_{13} and ϕ_{23} , and (ii) introduction of an additive term to A_3 in the denominator. One can see easily that this term is quite negligible if one refers to the value of N_g ($\approx 10^{13} \text{ cm}^{-3}$).

We now consider the analysis of the experimental data using Eq. (6). Because of experimental difficulties in determining the population of level 4 we do not measure R_{43} . However, since the energy defect ΔE_{34} is small (43 cm^{-1}), one can consider that Boltzmann equilibrium between these two levels is rapidly obtained. So, using Eq. (5) we can

write in this case

$$R_{31} = \frac{(N_g \bar{v} Q_{13} + \phi_{13}) + R_{21}(N_g \bar{v} Q_{23} + \phi_{23})}{N_g \bar{v}(Q_3 - Q_{34}) + A_3}. \quad (7)$$

The quantity $Q_3 - Q_{34}$ is the cross section for collisional depopulation of level 3 to all other levels except level 4. We can determine Q_{13} , Q_{23} , and $Q_3 - Q_{34}$ from the measurements of R_{31} and R_{32} as a function of rare-gas pressure in the following way:

(a) At very low pressure Eq. (6) reduces to $R_{31} = (N_g \bar{v} Q_{13} + \phi_{13})/A_3$, from which Q_{13} can be determined (a similar procedure allows the determination of Q_{23}).

(b) At higher pressure Eq. (7) is used to determine $Q_3 - Q_{34}$, providing a check on the Q_{13} and Q_{23} values. In fact, because of uncertainties associated with the values of R_{21} (and R_{12}) at high rare-gas pressure the value of $Q_3 - Q_{34}$ was determined only in the case of helium.

For different sets of parameters we compute the curves R_{31} and R_{32} as functions of rare-gas pressure to test the obtained values (Figs. 4 and 5). Finally, we remark that Boltzmann equilibrium at the gas temperature T for levels 3 and 4 is probably achieved in a rare-gas-pressure range when the denominator of Eq. (7) is dominated by A_3 .

The results that we obtained are shown in Table I. The values previously obtained for the $(1 \rightleftharpoons 2)$ transitions are also reported in this table, because they will be of interest for the discussion.

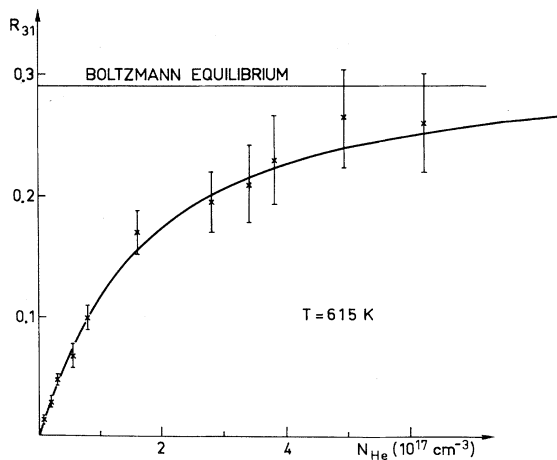


FIG. 4. Plot of the R_{31} population ratio against He pressure (ratio defined in the text). The theoretical value of R_{31} at Boltzmann equilibrium is shown. The experimental points are obtained by using Warner's A values (see text).

C. Uncertainties

1. Negligible effects

We will show first that some effects are not important when analyzing the experimental data.

Because the Doppler widths of the absorption lines involved in this experiment are narrower than the spectral width of the exciting line, there is no selection of the excited-cesium-atom velocities.

Polarization effects are not taken into account. No polarization systems are used for excitation and detection. However, the laser might exhibit a low degree of linear polarization. The excitation of the $7^2P_{1/2}$ level cannot produce population differences among the magnetic sublevels,¹⁸ and only a slight anisotropy can occur when pumping the $7^2P_{3/2}$ level. No variations in the experimental results are observed for different optical configurations of the laser. Moreover, the cross sections Q_{12} and Q_{21} , determined from separate measurements, are in good agreement with the principle of detailed balancing. We notice too that the measurements of R_{31} and R_{32} (determined when pumping either the $7^2P_{1/2}$ or the $7^2P_{3/2}$ level) are quite consistent. Thus our experimental cross sections are the sums of the cross sections for the individual Zeemann transitions of the $(J, m_j) - (J', m_{j'})$ type.

Previous experiments^{1,19} show that collisions with molecular gases may be important. We think that the high purity of the gas and the precautions taken when using it ensure that molecular impurities have no importance when measuring cross

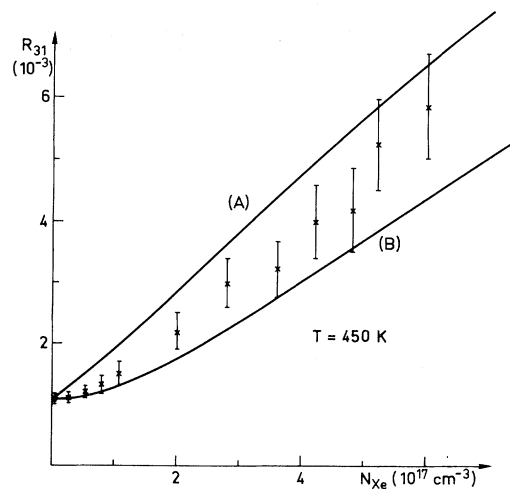


FIG. 5. Plot of the R_{31} population ratio against Xe pressure (ratio defined in the text). The two curves are computed by using Eq. (7) for $Q_{13} = 5 \times 10^{-3} \text{ \AA}^2$ (curve A) and $Q_{13} = 3 \times 10^{-2} \text{ \AA}^2$ (curve B).

TABLE I. Cross sections in Å². $\sum 6D_{3/2}$ represents the total collisional depopulation of the $6D_{3/2}$ level.

Transition	He	Ne	Ar	Kr	Xe
$T = 450 \text{ K}$					
$7P_{1/2} \rightarrow 7P_{3/2}$	(12±2)	(1.8±0.3)×10 ⁻¹	(1.2±0.2)×10 ⁻¹	(9.1±2.0)×10 ⁻²	(6.5±1.0)×10 ⁻¹
$7P_{3/2} \rightarrow 7P_{1/2}$	(11±2)	(1.6±0.3)×10 ⁻¹	(1.0±0.2)×10 ⁻¹	(7.7±1.7)×10 ⁻²	(5.7±1.0)×10 ⁻¹
$7P_{1/2} \rightarrow 6D_{3/2}$	(2.5±0.8)×10 ⁻¹	≤ 10 ⁻³	≤ 2×10 ⁻³	≤ 3·10 ⁻³	≥ 5·10 ⁻³ , ≤ 8×10 ⁻²
$7P_{3/2} \rightarrow 6D_{3/2}$	(2.7±0.8)×10 ⁻¹	(6±2)×10 ⁻⁴	(3.7±1.2)×10 ⁻³	(2.1±0.6)×10 ⁻²	(3.4±0.8)×10 ⁻¹
$\sum 6D_{3/2} \rightarrow (6D_{3/2} \rightarrow 6D_{5/2})$	(4.0±1.5)				
$T = 615 \text{ K}$					
$7P_{1/2} \rightarrow 7P_{3/2}$	(13±2)		(2.1±0.4)×10 ⁻¹		≥ 10 ⁻² , ≤ 7×10 ⁻²
$7P_{3/2} \rightarrow 7P_{1/2}$	(11±2)		(1.7±0.3)×10 ⁻¹		(7.5±1.5)×10 ⁻¹
$7P_{1/2} \rightarrow 6D_{3/2}$	(8±2)×10 ⁻¹				
$7P_{3/2} \rightarrow 6D_{3/2}$	(8±2)×10 ⁻¹				
$\sum 6D_{3/2} \rightarrow (6D_{3/2} \rightarrow 6D_{5/2})$	(6±2)				

sections greater than 10^{-19} cm^2 . Thus only the value obtained for Q_{23} in the case of neon could be significantly affected by residual molecular impurities.

The model used to determine the cross sections (see Sec. III B) assumes that no radiative cascade effect from upper levels exists. Ions, possibly created by the excitation process, could produce after recombination atomic excited levels. We verified by looking at transitions coming from upper levels that no cascade effect appeared under our experimental conditions.

2. Causes of experimental errors

The experimental errors come essentially from the determination of the ratios $N(i)/N(j)$ as given by Eq. (2) and the densities N_g and N_{Cs} .

(i) The uncertainty associated with the real counting rate is between 3 and 15%, taking into account a dead-time correction and statistical error. The calculation of the effect of light absorption has an uncertainty of 20%, mainly due to the uncertainty in the Cs density value. This absorption effect contributes only 20% in the determination of the X_j value. So we evaluate the error in X_j to be less than 5%. The coefficient Y_{ij} is more difficult to determine with accuracy. Its determination requires three steps: (a) The measurement of how light intensity is split between the sensitized-fluorescence and the direct-fluorescence channels; this ratio depends upon the geometrical arrangement of the two channels. The resulting uncertainty is the same as for the counting rate (about 10%). (b) The determination of the sensitivity as a function of wavelength of the channels, using a tungsten lamp. The resulting uncertainty does not exceed 5%. (c) The calibration of the neutral density filter used in the path of the direct fluorescence light. The uncertainty that results is less than 3%. Thus the determination of Y_{ij} is achieved with about 15% uncertainty. One can consider that the population ratio corresponding to an experimental point is known with 20–30% accuracy for a given set of A coefficients.

(ii) The pressure measurements are more accurate. The determination of the rare-gas pressure N_g , using a cathetometer, is made with great accuracy, and the thermal-transpiration correction is sufficiently elaborate to allow the determination of N_g with less than 5% uncertainty. A diffusion time sufficient to ensure pressure homogeneity in the measurement cell is necessary. An accurate determination of the cesium density is not required in our experiments as the rare-gas pressure determines the population ratios. The temperature regulation of the sidearm containing liquid cesium

ensures sufficient stability of the cesium density. However, the absolute value of N_{Cs} is not precisely known, leading, as noted previously, to an uncertainty in the determination of the X_j coefficient.

3. Estimation of errors concerning Q_{13} , Q_{23} , and Q_3-Q_{34}

We use the following procedure. A set of curves of R_{13} (and R_{23}) is plotted as a function of rare-gas pressure, for different values of the cross sections [Eqs. (6) and (7)]. By comparing these curves with the experimental points and their corresponding error bars, we determine the maximum error compatible with our measurements. This implies the validity of the model we have used to derive Eqs. (6) and (7). This point has been discussed in a previous section.

4. Choice of Einstein coefficients

We now discuss the choice of Einstein coefficients. Knowledge of these coefficients is required in each step of the interpretation of the experimental results: for the determination of the population ratios, the calculation of the light absorption correction, and the derivation of the cross sections. There are large discrepancies between the A values given by different authors (Table II). Consequently, systematic errors can result from the choice of a particular set of A values. It is therefore necessary at this point to state the set of A values we use and the reasons for our choice.

We discarded first the A coefficients given by Heavens²⁰ because they do not give Q_{12}/Q_{21} ratios in agreement with the principle of detailed balancing [Eq. (5)]. An accurate determination of this ratio requires knowledge of the ratio of the A coefficients for the ($7^2P_{3/2} \rightarrow 6^2S_{1/2}$) and ($7^2P_{1/2} \rightarrow 6^2S_{1/2}$) transitions with a sufficient accuracy. The values of this ratio, obtained when using separately the results of Stone,²¹ Warner,¹⁵ Norcross,²² and Weisheit,²³ are close, although the values obtained by these authors for each of the A coefficients differ significantly. Some experimental measurements of this ratio are also available.^{22,24,25} The average experimental value is about 2.45, which is close to the theoretical values given by the four authors previously quoted. Note that the

value obtained by Heavens is 1.40.

The problem of the choice of an A set is posed in a different way when considering the determination of Q_{13} and Q_{23} . The Einstein coefficients associated with the ($7^2P_{1/2} \rightarrow 6^2S_{1/2}$) and ($7^2P_{3/2} \rightarrow 6^2S_{1/2}$) transitions have been calculated by the previously quoted authors and the coefficients associated with the ($6^2D_{3/2} \rightarrow 6^2P_{1/2}$) transition only by Warner and Stone. To interpret the data we must know the ratios of ($A_{6^2D_{3/2} \rightarrow 6^2P_{1/2}}$) to ($A_{7^2P_{3/2} \rightarrow 6^2S_{1/2}}$) and ($A_{6^2D_{3/2} \rightarrow 6^2P_{1/2}}$) to ($A_{7^2P_{1/2} \rightarrow 6^2S_{1/2}}$). We calculated them from Warner and Stone's results; in the cases of Weisheit and Norcross we used A values for the ($6^2D_{3/2} \rightarrow 6^2P_{1/2}$) transition given by either Warner or Stone, which are close. The choice of the A set is made by comparison of the equilibrium ratios given by Eq. (5) and the experimental ratios R_{31} and R_{32} determined with the various sets of A values. The ratios should be very close to equilibrium values at high pressure of helium. The values of R_{31} and R_{32} can be seen as constant for helium pressure greater than 30 Torr (the higher-pressure measurements are performed at about 45 Torr). In these experimental conditions R_{31} and R_{32} are derived only by using Eq. (2), without reference to any model, providing a direct measurement of the ratio of the two corresponding A values. The Warner coefficients provide the best agreement for the R_{31} and R_{32} values (Fig 4). It should be mentioned that in the case of the measurements of R_{12} and R_{21} at high pressure of helium all the systems, except Heavens's, gave reasonable agreement with the experimental measurements.

Note that the theoretical lifetimes of both the $7^2P_{3/2}$ and $7^2P_{1/2}$ levels, calculated using Warner's values, are also in good agreement with the experimental determination.²⁶⁻²⁸ As far as we know, no measurements of the $6^2D_{3/2}$ lifetime have been reported.

For all these reasons we use Warner's A values for the analysis of our experimental data.

IV. DISCUSSION

Previous experimental results concerning the collisional transitions between $^2P_{1/2}$ and $^2P_{3/2}$ levels of the alkali metals, show clearly that the values for the cross sections, for a given rare-gas

TABLE II. Theoretical values of Einstein's A coefficients (10^6 sec^{-1}).

Transition	Ref. 20	Ref. 21	Ref. 15	Ref. 23	Ref. 22
$7P_{1/2} \rightarrow 6S_{1/2}$	2.12	0.90	1.58	0.65	0.76
$7P_{3/2} \rightarrow 6S_{1/2}$	2.97	2.79	4.18	1.69	1.67
$6D_{3/2} \rightarrow 6P_{1/2}$	12.7	12.9	9.86		

TABLE III. Experimental cross sections (\AA^2) for various fine-structure collisional transitions.

	ΔE (cm^{-1})	T (K)	He	Ne	Ar	Kr	Xe	References	
Na	$3P_{1/2} \rightarrow 3P_{3/2}$	17	397	86	67	110	85	89.8	4
K	$4P_{1/2} \rightarrow 4P_{3/2}$	58	368	59.5	14.3	36.7	61.4	104	4
Rb	$6P_{1/2} \rightarrow 6P_{3/2}$	77	430	29.3	10.3	24	23.3	43.9	2
Cs	$8P_{1/2} \rightarrow 8P_{3/2}$	83	420	34	4.4	5.5	4.5	15	1
Cs	$7P_{1/2} \rightarrow 7P_{3/2}$	181	450	12	1.8×10^{-1}	1.2×10^{-1}	9.1×10^{-2}	6.5×10^{-1}	5
Rb	$5P_{1/2} \rightarrow 5P_{3/2}$	238	450	1×10^{-1}	4×10^{-3}	1×10^{-3}	5×10^{-4}	6×10^{-4}	29
Cs	$6P_{1/2} \rightarrow 6P_{3/2}$	554	450	1.5×10^{-4}	4×10^{-6}				29

atom, decrease with increasing energy defect ΔE (see Table III). However, the variation of the cross-section values as a function of the energy defect is found to be different for each rare-gas atom. Therefore reference to the energy defect alone is insufficient for the discussion of the values of the experimental cross sections. The cross sections obviously depend on the forces of interaction between the rare-gas and alkali atoms. The nature of the rare-gas atom and the positions of the initial and final levels in the energy diagram of the alkali atom therefore have to be considered.

Theoretical calculations of the intramultiplet-transition cross sections have previously been carried out for the first resonant doublets of the alkali metals.⁶⁻⁸ Good agreement was obtained in the case of the lightest alkali metals, for which the energy defect involved in the transition is small. These calculations generally used adiabatic potential curves which have been obtained asymptotically and did not take into account possible coupling with neighboring levels. Thus these potential-energy curves did not show any structure. Simplified potential-energy curves have also been used for the determination of intramultiplet transitions in the third resonant doublet of cesium,³ but no agreement has been obtained between theory and experiment.¹ As far as we know, no calculation of cross sections concerning both the intra- and intermultiplet processes associated with the four levels considered here has been carried out. Recently, extensive molecular potentials for the alkali metal-rare-gas-atom pairs have been calculated.^{9,10} They are correlated at large internuclear distances with numerous excited levels of the alkali metals. The adiabatic potential-energy curves generally show a structure, more or less pronounced, according to the alkali-metal-rare-gas-atom pair which is considered (see, for example, Fig. 6). This structure is clearly demonstrated to be due to coupling between neighboring levels. Because the other resonant doublets are more isolated from the first levels than the higher excited 2P doublets, the corresponding adiabatic potential-energy curves are seen to be more regu-

lar, with, however, some structure. A calculation of the intramultiplet cross sections, using these potential curves, is in progress.

Let us consider now the results obtained for the intermultiplet

$$(^7P_{1/2} \xrightarrow{Q_{13}} 6^2D_{3/2})$$

and

$$(^7P_{3/2} \xrightarrow{Q_{23}} 6^2D_{3/2})$$

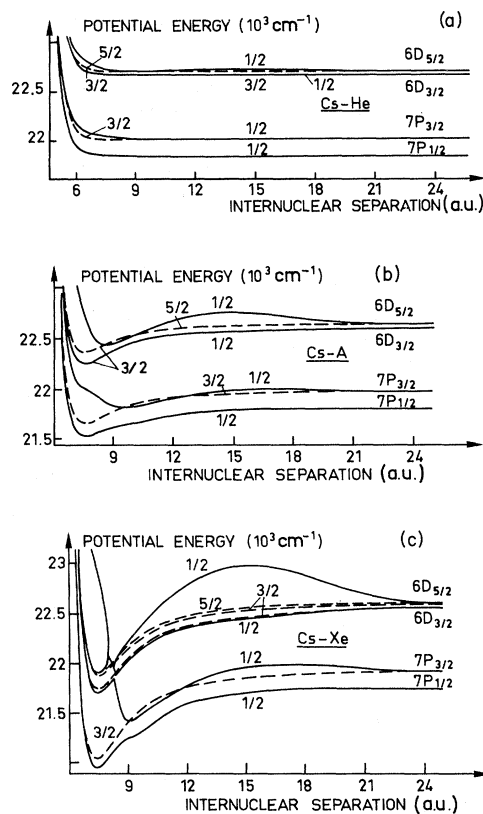


FIG. 6. Potential-energy curves that correlate asymptotically with the $7P_{1/2}$, $7P_{3/2}$, $6D_{3/2}$, and $6D_{5/2}$ states of cesium, taken from Ref. 10. A full discussion of these curves is found in Ref. 9. (a) Cs-He; (b) Cs-Ar; (c) Cs-Xe.

transitions. Two main points appear: (a) The experimental values of Q_{23} are much higher than those obtained for fine-structure transitions with about the same energy defect (in our case $\Delta E = 640 \text{ cm}^{-1}$). (b) The ratio Q_{13}/Q_{23} is quite different when considering the case of helium or of krypton and xenon (for neon and argon it is impossible to give a conclusion.)

In the cases of helium and neon, Gallagher²⁹ has done a detailed study of the temperature dependence of the intramultiplet transitions within the first 2P doublet of cesium (the fine-structure splitting is 554 cm^{-1}). At 448 K the cross sections for helium and neon were found to be about 10^{-21} and 10^{-22} cm^2 , respectively. In our case, for an energy defect of 640 cm^{-1} , we obtain 2.7×10^{-17} and $6 \times 10^{-20} \text{ cm}^2$. For the other rare-gas atoms, an extrapolation of the measurements done by the group at Windsor University⁴ leads also to cross sections two to four orders of magnitude lower than those obtained here. If we examine the adiabatic potential-energy curves asymptotically correlated with the 2 and 3 levels, we observe a certain structure due to coupling between levels (Fig. 6). This structure is more pronounced and localized when the mass of the rare-gas atom increases. For the xenon case the corresponding curves show a very pronounced avoided crossing. Except for helium, the magnitudes of the cross sections seem clearly related to the structure of the potential-energy curves. In the case of helium the curves are regular; the large value of the measured cross section probably indicates that the interaction during the collision takes place over a large range of internuclear distances. A similar effect arises in the case of the first resonant doublet of the alkali metals.

An estimate of the Q_{23} cross section by Landau-Zener theory has been carried out for the xenon case, using the potential curves of Ref. 10. Two curves of the same symmetry, asymptotically correlated to the 2 and 3 levels, show a pronounced avoided crossing for an internuclear distance R_c of about 8 a.u., allowing the determination of the Landau-Zener transition probability at this point.^{30,31} This probability depends, in particular, on the energy defect ΔU between the curves at the pseudocrossing point and also on the absolute value of the slope difference ΔF of the curves at R_c . After averaging the calculated cross sections over a Maxwellian velocity distribution, and taking into account the multiplicity of the considered levels, the theoretical averaged cross sections are in reasonable agreement with the experimental values (curve A in Fig. 7). Contribution of the avoided crossing between the potential curves of the same symmetry correlated with the 1 and 2 levels has

been found to be negligible. It is seen in Fig. 6 that two potential-energy curves of different symmetry are correlated with the level 3 and cross at an internuclear distance very close to R_c . It is possible, because of rotational coupling, to go from the potential curve associated with level 2 to that associated with level 3, after passing through the avoided crossing at R_c . Using a simplified four-level basis for the computation of the adiabatic potential curves, we have estimated this rotational coupling at the crossing point.

The calculation shows that the effect of the rotational coupling is quite negligible for the determination of the Q_{23} cross-section value. The results are shown in Fig. 7 (curve B). The difference between the two calculations is essentially due to the fact that the calculation of the Landau-Zener probability is very sensitive to the values of the parameters ΔU and ΔF ; in fact, they are different when using potential curves taking into account either a reduced basis (levels 1, 2, 3, and 4) or a larger one.⁹ However, these two theoretical estimations of the Q_{23} cross section are in reasonable agreement with the experimental results both for the order of magnitude and the temperature dependence. A more complete calculation, using the potential curves and taking into account their whole structure, is in progress. It will permit a general comparison between theory and experiment in the case of each rare gas and particularly in the case of helium.

The adiabatic potential-energy curves permit also a discussion of the second point mentioned above. For the case of helium the curves associated with the levels 1, 2, and 3 are smooth and parallel along a large range of internuclear distance; the values of the cross sections Q_{13} and Q_{23} are found experimentally to be very close to each other. We can therefore reasonably expect in this case that the interaction would take place

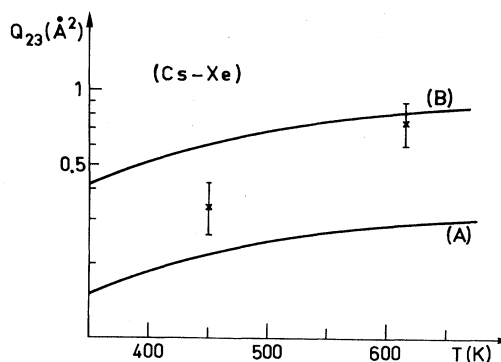


FIG. 7. Comparison between theory and experiment of the cross section for the $(7P_{3/2} \rightarrow 6D_{3/2})$ transition in the (Cs-Xe) case (notation defined in the text).

over a large range of internuclear distance for both the 1 → 3 and 2 → 3 transitions. For xenon and krypton the curves associated with the levels 1, 2, and 3 show structure. Moreover, the structure is different when considering the curves associated with the levels 1 and 2. In these cases the cross sections Q_{13} and Q_{23} are found experimentally to be very different. In the case of xenon, where an avoided crossing at about 9.25 a.u. is seen between the same symmetry curves associated with the levels 1 and 2, it has been possible to estimate theoretically the cross section Q_{13} . This has been done, as before, taking into account the avoided crossings shown by the potential-energy curves associated with levels 1 and 2 and 2 and 3, respectively. The theoretical results are in good agreement with the experimental estimates (Fig. 8).

It is clear that our analysis of the results concerning intermultiplet transitions is essentially based on the structure of the potential curves involved in the transition. The same analysis for any intramultiplet transition might be used if the corresponding curves show such structure.

The last point to be discussed is the value obtained for $Q_3 - Q_{34}$ in the case of helium. We can write

$$Q_3 - Q_{34} = Q_{31} + Q_{32} + Q_q,$$

where Q_q represents the collisional depopulation of level 3 to all levels other than those considered here (levels 1, 2, and 4). Using the principle of detailed balancing we can calculate $Q_{31} + Q_{32}$ from our results and compare the value obtained with $Q_3 - Q_{34}$. This permits an estimate of Q_q . One can see that no collisional depopulation of level 3 to any level other than 1, 2, or 4 occurs. It is well known that large "quenching" cross sections are obtained in the case of a molecular-perturber gas (in particular, nitrogen).^{1,19} Moreover, a theoretical calculation using simplified potential curves has predicted large "quenching" cross sections for highly excited alkali-metal atoms colliding with rare-gas atoms.³ The fact that the (Cs-He) potential-energy curves have no localized structure does not permit a conclusion before a more complete calculation is performed. For the other rare gases at thermal energies the potential curves show only coupling between the four levels considered here. Thus it appears that the corresponding cross sections Q_q would probably be small.

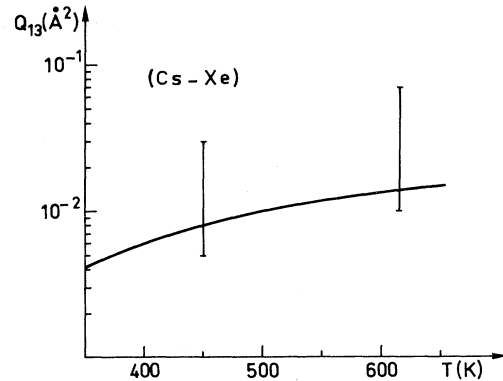


FIG. 8. Comparison between theory and experiment of the cross section for the ($7P_{1/2} \rightarrow 6D_{3/2}$) transition in the (Cs-Xe) case (notation defined in the text).

V. CONCLUSION

This experimental study of inelastic collisional processes involving 7^2P and 6^2D cesium atoms and ground-state rare-gas atoms at thermal energies leads to surprising results if one considers only the energy defect for these processes. However, if the experimental results are discussed using the theoretical adiabatic potential-energy curves obtained recently, a satisfactory explanation of the main features of this work is obtained. The potential curves show various structures due to coupling between neighboring levels. The structure is of different importance for different rare-gas atoms. This explains (a) the possibility of having a large cross section, even in the case of a large energy defect between the considered levels, and (b) the dependence of the Q_{13}/Q_{23} ratio on the nature of the rare gas.

In the case of the (Cs-Xe) pair the potential-energy curves show two pronounced avoided crossings. By using the Landau-Zener formula to evaluate the transition probabilities at these points, the Q_{13} and Q_{23} cross sections are found to be in reasonable agreement with the experimental values. This provides a first check of the reliability of the theoretical potential curves, the accuracy of which was difficult to determine *a priori*.

ACKNOWLEDGMENT

We wish to thank Dr. P. M. Stone for a critical reading of the manuscript.

- ¹M. Pimbert, *J. Phys. (Paris)* **33**, 331 (1972).
- ²I. Siara, E. S. Hrycyshyn, and L. Krause, *Can. J. Phys.* **50**, 1828 (1972).
- ³E. E. Nikitin and A. J. Reznikov, *Chem. Phys. Lett.* **8**, 161 (1971).
- ⁴P. L. Lijnse, in Report No. 398, *Fysisch Laboratorium, Rijksuniversiteit Utrecht*, 1972 (unpublished), and references therein.
- ⁵J. Cuvellier, P. R. Fournier, F. Gounand, and J. Berlande, *C. R. Acad. Sci. B* **276**, 855 (1973).
- ⁶E. I. Dashevskaya and E. E. Nikitin, *Opt. Spektrosk.* **22**, 866 (1967) [*Opt. Spectrosc.* **22**, 473 (1967)].
- ⁷E. I. Dashevskaya, E. E. Nikitin, and A. I. Reznikov, *Opt. Spektrosk.* **29**, 1016 (1970) [*Opt. Spectrosc.* **29**, 540 (1970)].
- ⁸F. Masnou-Seeuws, *J. Phys. B* **3**, 1437 (1970).
- ⁹J. Pascale and J. Vandeplanque, *J. Chem. Phys.* **60**, 2278 (1974).
- ¹⁰J. Pascale and J. Vandeplanque, Commissariat à l'Énergie Atomique Report (unpublished) (available on request from the present authors).
- ¹¹W. B. Nottingham, Thermo-Electron Engineering Corporation Technical Report No. TEE 7002-5, 1960 (unpublished); see also Ref. 1.
- ¹²J. L. Lemaire and F. Rostas, *J. Phys. B* **4**, 555 (1971).
- ¹³F. Lambert, *C. R. Acad. Sci. B* **274**, 1406 (1972).
- ¹⁴Y. V. Evdokimov, *Opt. Spektrosk.* **24**, 832 (1968) [*Opt. Spectrosc.* **24**, 448 (1968)].
- ¹⁵T. H. Warner, *Mon. Not. R. Astron. Soc.* **139**, 115 (1968).
- ¹⁶T. Edmonds and J. P. Hobson, *J. Vac. Sci. Technol.* **2**, 182 (1965).
- ¹⁷E. H. Kennard, *Kinetic Theory of Gases* (McGraw-Hill, New York, 1938).
- ¹⁸G. W. Series, *Rep. Prog. Phys.* **22**, 280 (1959).
- ¹⁹J. L. Rocchiccioli, *C. R. Acad. Sci. (Paris)* **274**, 787 (1972).
- ²⁰O. S. Heavens, *J. Opt. Soc. Am.* **51**, 1058 (1961).
- ²¹P. M. Stone, *Phys. Rev.* **127**, 1151 (1962).
- ²²D. W. Norcross, *Phys. Rev. A* **7**, 606 (1973); and references therein.
- ²³J. C. Weisheit, *Phys. Rev. A* **5**, 1621 (1972).
- ²⁴L. Agnew, *Bull. Am. Phys. Soc.* **11**, 327 (1966).
- ²⁵R. J. Exton, dissertation (West Virginia University, 1972) (unpublished).
- ²⁶R. W. Schmieder, A. Lurio, and W. Happer, *Phys. Rev. A* **2**, 1216 (1970).
- ²⁷E. L. Altmann and S. A. Kazantsev, *Opt. Spektrosk.* **28**, 805 (1970) [*Opt. Spectrosc.* **28**, 432 (1970)].
- ²⁸E. L. Altmann and M. Chaika, *Opt. Spektrosk.* **19**, 968 (1965) [*Opt. Spectrosc.* **19**, 538 (1965)].
- ²⁹A. Gallagher, *Phys. Rev.* **172**, 88 (1968).
- ³⁰C. Zener, *Proc. R. Soc. A* **137**, 696 (1932); L. D. Landau, *Phys. Z. Sowjetunion* **2**, 46 (1932).
- ³¹L. Landau and L. Lifschitz, *Quantum Mechanics* (Pergamon, London, 1958).